Article

In Situ Observation of the Internal Structure and Composition of Biomineralized *Emiliania huxleyi* Calcite by Solid-State NMR Spectroscopy

Ronen Gertman, Ira Ben Shir, Shifi Kababya, and Asher Schmidt

J. Am. Chem. Soc., **2008**, 130 (40), 13425-13432 • DOI: 10.1021/ja803985d • Publication Date (Web): 10 September 2008

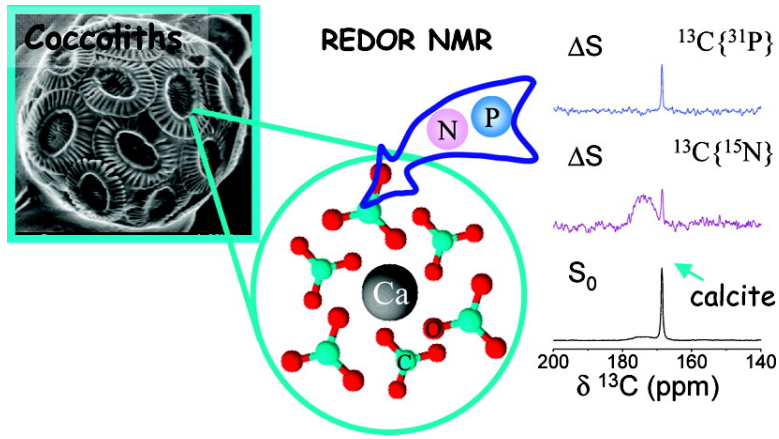

More About This Article

Additional resources and features associated with this article are available within the HTML version:

- Supporting Information
- Access to high resolution figures
- Links to articles and content related to this article
- Copyright permission to reproduce figures and/or text from this article

View the Full Text HTML

J|A|C|S
ARTICLES

Published on Web 09/10/2008

In Situ Observation of the Internal Structure and Composition of Biomineralized *Emiliania huxleyi* Calcite by Solid-State NMR Spectroscopy

Ronen Gertman, Ira Ben Shir, Shifi Kababya, and Asher Schmidt*

Schulich Faculty of Chemistry and the Russell Berrie Nanotechnology Institute, Technion−Israel Institute of Technology, Haifa 32000, Israel

Received May 28, 2008; E-mail: chrschm@tx.technion.ac.il

Abstract: Biomineralization, particularly the formation of calcium carbonate structures by organisms under ambient conditions, is of vast fundamental and applied interest. Organisms finely control all aspects of the formation of the biomaterials: composition, polymorph, morphology, and macroscopic properties. While *in situ* molecular-level characterization of the resulting biominerals is a formidable task, solid-state magic angle spinning NMR is one of the most powerful analytical techniques for this purpose. It is employed in this study to elucidate the structure and composition of biogenic calcite formed by *Emiliania huxleyi*, a unicellular alga distinguished by its exquisitely sculptured calcite cell coverings known as coccoliths. Strain 371 (CCMP) was grown and harvested from ^{15}N- and ^{13}C-enriched growth medium, with biosynthetic labeling to enhance the sensitivity of the NMR measurements. Crystalline and interfacial calcite environments were selectively probed using direct and indirect (cross-polarized) ^{13}C excitation, respectively. Different crystalline environments, in particular structural defect sites at concentrations of up to 1.4% with P and N moieties incorporated, were identified using ^{13}C rotational-echo double-resonance (REDOR) NMR. REDOR-derived geometrical constraints show that the P and N atoms at the defect sites are 3.2 and 2.3 (±0.2) Å apart from a crystalline carbon carbonate. The phosphorus and nitrogen moieties within the biogenic calcite are identified as small, non-protonated moieties, attributed to inorganic ions such as PO_4^{3-} and NO_3^-. The carbonates adjacent to these defects are chemically indistinguishable from bulk crystalline carbonates, yet their immediate environments experience reduced rigidity, as reflected by substantial $T_1(^{13}CO_3^{2-})$ shortening. Interfacial carbonates, on the other hand, reside in structurally/chemically perturbed environments, as reflected by heterogeneous line broadening. This study is the first to directly unravel evidence on the incorporation of P/N moieties as structural defects within *E. huxleyi* biogenic calcite, and on the state of the adjacent crystalline carbonates.

Introduction

Biomineralization in general, and particularly formation of calcium carbonate ($CaCO_3$) structures by organisms at ambient conditions, poses vast interest regarding the control exercised by the organism over the resulting polymorph (e.g., calcite, aragonite), composition, fine structure, morphology, and macroscopic properties.[1−5] While understanding of the molecular and cellular mechanisms underlying the formation of inorganic materials begins to unfold,[1,6−11] much still remains obscure, and its elucidation requires varied studies. The fundamental understanding of biomineralization processes and the characterization of the resulting inorganic materials each sets a prime goal on its own. Achieving these goals is crucial when tailored design of functional materials that utilize nature's optimized processes is desired. Materials design capabilities that may emerge span diverse applications in biomedicine, biocompatibility, nanoelectronic devices, and biotechnology.[12−16]

Emiliania huxleyi is a unicellular alga (phytoplankton), distinguished by its exquisitely sculptured calcium carbonate cell coverings, known as coccoliths.[1,4,5,17] It is found throughout the world's oceans and considered the world's major producer

(1) Young, J. R.; Davis, S. A.; Bown, P. R.; Mann, S. *J. Struct. Biol.* **1999**, *126*, 195–215.
(2) Henriksen, K.; Stipp, S. L. S.; Young, J. R.; Marsh, M. E. *Am. Mineral.* **2004**, *89*, 1709–1716.
(3) Saruwatari, K.; Ozaki, N.; Nagasawa, H.; Kogure, T. *Am. Mineral.* **2006**, *91*, 1937–1940.
(4) Dove, P. M., De Yoreo, J. J., Weiner, S., Eds. *Biomineralization*; Reviews in Mineralogy and Geochemistry *54*; Mineralogical Society of America: Washington, DC, 2004.
(5) Mann, S. *Biomineralization: Principles and Concepts in Bioinorganic Materials Chemistry*; Oxford University Press: New York, 2001.
(6) De Jong, E.; Van Rens, L.; Westbroek, P.; Bosch, L. *Eur. J. Biochem.* **1979**, *99*, 559–567.
(7) Shiraiwa, Y. *Comp. Biochem. Phys. B* **2003**, *136*, 775–783.
(8) Marsh, M. E. *Comp. Biochem. Phys. B* **2003**, *136*, 743–754.
(9) Sato, K.; Kumagai, Y.; Kogure, T.; Watari, K.; Tanaka, J. *J. Ceram. Soc. Jpn.* **2006**, *114*, 754–759.
(10) Addadi, L.; Raz, S.; Weiner, S. *Adv. Mater.* **2003**, *15*, 959–970.
(11) DeOliveira, D. B.; Laursen, R. A. *J. Am. Chem. Soc.* **1997**, *119*, 10627–10631.
(12) Camprasse, G.; Camprasse, S.; Gill, G. A. *C. R. Acad. Sci. III−VIE* **1988**, *307*, 485–491.
(13) Piattelli, A.; Podda, G.; Scarano, A. *Biomaterials* **1997**, *18*, 623–627.
(14) Remes, A.; Williams, D. F. *Biomaterials* **1991**, *12*, 661–667.
(15) Stupp, S. I.; Braun, P. V. *Science* **1997**, *277*, 1242–1248.
(16) Walsh, D.; Mann, S. *Nature* **1995**, *377*, 320–323.
(17) Laguna, R.; Romo, J.; Read, B. A.; Wahlund, T. M. *Appl. Environ. Microbiol.* **2001**, *67*, 3824–3831.

of calcite.[18] *E. huxleyi* is one of the most studied coccolithophore species, and its wide tolerance to ecological changes and rapid growth made it an excellent candidate for biomineralization research. In turn, *E. huxleyi* serves as a platform to investigate functional control and regulation and their dependencies on environmental factors such as nutrient concentration and temperature.[19−22]

The incorporation of biomolecules into the biomineralized calcium carbonate lattice has been assumed for a long time.[5] Evidence of the presence of calcite-associated bioorganics has also been reported.[2,23] However, evidence is often obtained by disintegrating the inorganics and identifying the released molecules.[24−28] Obviously, such evidence cannot provide an *in situ* molecular-level description of the state of such molecules within or around the biomineral. In both cases diffraction techniques fall short, unable to focus on the sites of interest which are sparse and may also present reduced local order. The quest for knowledge of the bioorganic−inorganic interface with molecular-level details therefore faces severe obstacles. Solid-state NMR techniques are best suited to address such goals. To exploit the strength of solid-state NMR, its inherently low sensitivity must be enhanced. The latter is achieved in our study by the biosynthetic incorporation of the stable isotopes ^{13}C and ^{15}N from the enriched growth media. We have applied ^{13}C, ^{15}N, and ^{31}P solid-state NMR techniques to such enriched *E. huxleyi* samples to elucidate the structure and composition of the biogenic inorganic $CaCO_3$ as formed by *E. huxleyi*. This allowed, for the first time, the characterization of the chemical environments of the biogenic $CaCO_3$ *in situ*, both the bulk crystalline and the interfacial regions as well as the bioorganic components.

Experimental Section

Culture and Sample Preparation. *E. huxleyi*, strain 371, f/2 culture medium kit, and natural seawater were purchased from Bigelow Laboratory (West Boothbay Harbor, ME) and prepared according to f/2 medium kit recipes.[29,30] Final growth medium was prepared using 98% ^{15}N-enriched $Na^{15}NO_3$ (instead of the natural abundance $NaNO_3$, of the f/2 kit) and 25% ^{13}C-enriched $NaH^{13}CO_3$.[31] $NaNO_3$, $NaHCO_3$, and NaH_2PO_4 were added to the natural seawater to establish minimum concentrations of 8.84×10^{-4}, 2.07×10^{-3}, and 3.63×10^{-5} M, respectively. Both stable isotope-labeled salts were purchased from Cambridge Isotope Laboratories (Andover, MA) at enrichment levels of 98%. The cultures were grown in an Innova-44 shaker−incubator, 800−1200 mL culture solution in 3 L Erlenmeyer glass flasks, with 13/11 h light/dark cycle, at 18 °C and 80 rpm. The cultures were harvested after a growth period of 4−8 weeks by centrifuging for 10 min at 15180*g*, washing with double-distilled water (ddH_2O) and recentrifuging three times, and finally lyophilizing overnight. Samples prepared as described were denoted *intact*. To remove excess bioorganic matter, the content harvested by centrifugation and a single wash was immersed in 2.5% sodium hypochlorite (in 10 mL ddH_2O) for 1 h while stirring, followed by three centrifuge−wash cycles and finally lyophilization. Samples so prepared were named *treated*. About 100 mg lyophilized samples were obtained by harvesting 0.5 and 1 L for the intact and treated preparations, respectively. For the NMR measurements, about 65−100 mg portions of the lyophilized samples were packed into 5 mm zirconia rotors with Teflon plugs and Vespel drive tips. In addition, *E. huxleyi* was also grown with the f/50 culture medium kit, a poor medium in which nutrient concentration is 25-fold lower than that of f/2. Over 10 samples were prepared starting from culture growth and subjected to NMR and microscopy characterization, confirming reproducibility.

Solid-State NMR. NMR spectroscopy measurements were carried out on a Chemagnetics/Varian 300 MHz CMX-infinity solid-state NMR spectrometer equipped with three radio frequency channels and a 5 mm triple-resonance APEX Chemagnetics probe using 5 mm zirconia rotors. Samples were spun at 5000 ± 2 Hz and maintained at 4 ± 0.1 °C throughout the experiments. Cross-polarization magic angle spinning (CPMAS) echo experiments (indirect excitation) were carried out with 5.0 μs $\pi/2$, 10.0 μs π pulse widths, an echo interval τ (200 μs) identical to the rotor period T_R, a ^1H decoupling level of 100 kHz, and a relaxation delay of 2 s; Hartmann−Hahn rf levels were matched at 50 kHz with contact times of 2 ms for ^{15}N and ^{13}C and 0.7 ms for ^{31}P. ^{13}C CPMAS was also conducted with 8 ms contact time.

Direct ^{13}C excitation echo experiments (DE) were carried out with 5.0 μs $\pi/2$, 10.0 μs π pulse widths, an echo interval τ equal to the rotor period T_R (200 μs), a ^1H decoupling level of 100 kHz, and relaxation delays of 20, 2400, and 4000 s.

$^{13}C\{^{31}P\}$ and $^{13}C\{^{15}N\}$ rotational-echo double-resonance (REDOR) experiments were conducted using a REDOR pulse sequence with refocusing π pulses on each rotor period (T_R) on the observe channel and dephasing π pulses in the middle of each rotor period on the nonobserved nuclei, followed by an additional two rotor periods with a chemical shift echo π pulse in the middle. REDOR π pulses employed xy8 phase cycling for the refocusing and recoupling pulses.[32,33] Data acquisition employed an alternating block mode, collecting a single S_0 transient with recoupling pulses turned off, followed by S_R transient collection with recoupling pulses turned on. REDOR difference data obtained via $S_0 - S_R$ subtraction, ΔS, yield spectra which exhibit peaks of dipolar-coupled chemical species exclusively. REDOR experiments were performed using both CP and DE excitation schemes, denoted CP-REDOR and DE-REDOR, respectively, each employing the respective experimental parameters. The number of collected transients was set to yield the desired signal-to-noise ratio. Typical numbers are 40960 for ^{13}C CP and CP-REDOR, 2560 for DE and DE-REDOR with 20 s, and about 50 for 40 and 67 min relaxation delays. All NMR measurements were carried out with sample temperature maintained at 4 °C.

The chemical shifts of ^{15}N, ^{13}C, and ^{31}P are reported relative to solid $(^{15}NH_4)_2SO_4$, TMS, and 85% H_3PO_4, respectively. The accuracy of the chemical shift determination for the CP and DE experiments is ±0.3 and ±0.1 ppm, respectively. Simulations and

(18) Westbroek, P.; Dejong, E. W.; Vanderwal, P.; Borman, A. H.; Devrind, J. P. M.; Kok, D.; Debruijn, W. C.; Parker, S. B. *Philos. Trans. R. Soc. B* **1984**, *304*, 435–443.
(19) Sorrosa, J. M.; Satoh, M.; Shiraiwa, Y. *Mar. Biotechnol.* **2005**, *7*, 128–133.
(20) Xu, Y.; Wahlund, T. M.; Feng, L.; Shaked, Y.; Morel, F. M. M. *J. Phycol.* **2006**, *42*, 835–844.
(21) Batvik, H.; Heimdal, B. R.; Fagerbakke, K. M.; Green, J. C. *Eur. J. Phycol.* **1997**, *32*, 155–165.
(22) Lessard, E. J.; Merico, A.; Tyrrell, T. *Limnol. Oceanogr.* **2005**, *50*, 1020–1024.
(23) Marsh, M. E.; Ridall, A. L.; Azadi, P.; Duke, P. J. *J. Struct. Biol.* **2002**, *139*, 39–45.
(24) Takahashi, K.; Yamamoto, H.; Onoda, A.; Doi, M.; Inaba, T.; Chiba, M.; Kobayashi, A.; Taguchi, T.; Okamura, T.; Ueyama, N. *Chem. Commun.* **2004**, 996–997.
(25) Pokroy, B.; Fitch, A. N.; Lee, P. L.; Quintana, J. P.; Caspi, E. N.; Zolotoyabko, E. *J. Struct. Biol.* **2006**, *153*, 145–150.
(26) Pokroy, B.; Fitch, A. N.; Marin, F.; Kapon, M.; Adir, N.; Zolotoyabko, E. *J. Struct. Biol.* **2006**, *155*, 96–103.
(27) Jaeger, C.; Groom, N. S.; Bowe, E. A.; Horner, A.; Davies, M. E.; Murray, R. C.; Duer, M. *Chem. Mater.* **2005**, *17*, 3059–3061.
(28) Feng, J.; Lee, Y. J.; Kubicki, J. D.; Reeder, R. J.; Phillips, B. L. *Magn. Reson. Chem.* **2008**, *46*, 408–417.
(29) Guillard, R. R. L. *Cult. Mar. Invertebr. Anim.* **1975**, 26–60.
(30) Guillard, R. R.; Ryther, J. H. *Can. J. Microbiol.* **1962**, *8*, 229–239.
(31) Berges, J. A.; Franklin, D. J.; Harrison, P. J. *J. Phycol.* **2001**, *37*, 1138–1145.
(32) Gullion, T.; Baker, D. B.; Conradi, M. S. *J. Magn. Reson.* **1990**, *89*, 479–484.
(33) Gullion, T.; Schaefer, J. *J. Magn. Reson.* **1989**, *81*, 196–200.

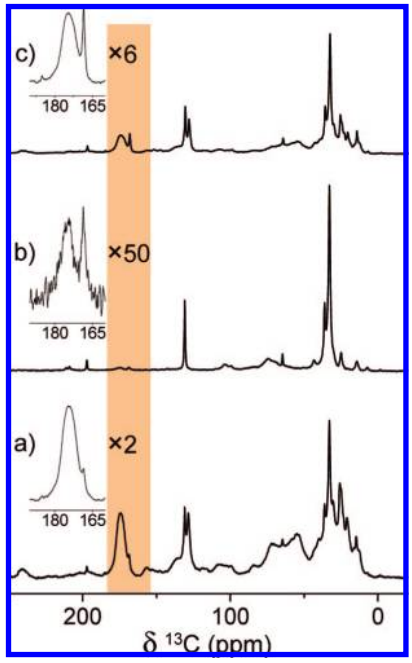

Figure 1. 75.5 MHz ^{13}C CPMAS NMR spectra of *E. huxleyi* samples. (a) Intact and (b) treated. A 2 ms CP contact time was used for both samples. (c) Intact, 8 ms contact time. At this long contact time, peaks of species with long $T_{1\rho}$ (such as carbonate) survive. The insets show an expanded view of the carboxylate−amide−carbonate region with the calcite carbonate peak at 168.6 ppm.

fitting of REDOR data were performed using SpinEvolution.[34] Peak areas were calculated by deconvolution using DMFIT.[35]

Microscopy. Both LEO Gemini 982 HRSEM and Leica light microscopes were used to track culture vitality and intactness. For the LEO HRSEM, the samples were dried on a commercial silicon wafer (TED PELLA); micrographs were obtained at low voltage, 3−4 kV, and magnification of up to 30000×.

Results

***E. huxleyi* NMR Characterization.** Intact samples, harvested from *E. huxleyi* grown on ^{13}C- and ^{15}N-enriched medium, were first characterized by ^{13}C, ^{15}N, and ^{31}P CPMAS NMR measurements. The cross-polarization technique enhances the signals of rare nuclei such as ^{13}C, ^{15}N, and ^{31}P by transferring the high polarization stored in the abundant, high-γ hydrogen atoms to these nuclei, yielding spectra in which hydrogen-rich environments are selected. Peak intensities in the resulting CP spectra depend on proximate hydrogen atoms, rendering them nonquantitative. This technique is used to probe primarily the bioorganic content of samples and the interfacial inorganic matter. Quantitative spectral evaluation utilizes DE MAS NMR measurements that require long relaxation delays, as dictated by the longest T_1 relaxation times of the observed type of nuclei (e.g., ^{13}C, ^{15}N, or ^{31}P). DE compared to CP measurements are therefore time-consuming and often less sensitive; in addition to signal enhancement, CP benefits also from the much shorter $T_1(^1\mathrm{H})$.

Carbon Content in *E. huxleyi* Samples. The ^{13}C CPMAS NMR spectrum of an intact *E. huxleyi* sample shown in Figure 1 a depicts the bioorganic content of the sample. Focus is drawn

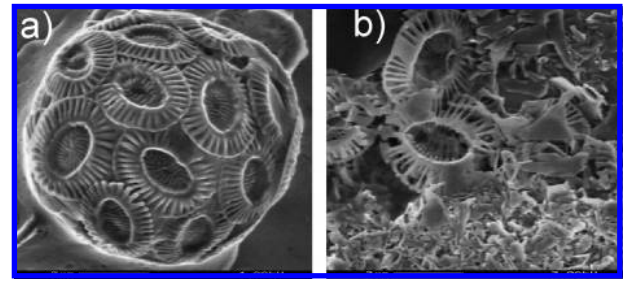

Figure 2. HRSEM images (magnification of 10000×) of *E. huxleyi* samples. (a) Intact, showing a whole cell surrounded by coccoliths. (b) Treated, showing coccoliths fragments.

to the carbonyl region at 160−190 ppm (Figure 1a, inset). The intense, broad peak at 175 ppm is attributed predominantly to the amide and carboxylate carbons that originate from the bioorganic content of the *E. huxleyi* cells. The relatively sharp, high-field shoulder at 168.6 ppm is attributed to the inorganic carbonate carbon of the calcite that makes up the coccoliths of the *E. huxleyi*. In order to further isolate inorganic content for its characterization, excess bioorganic matter was removed by a gentle treatment with NaOCl, sample named "treated". Typical HRSEM micrographs of intact samples (Figure 2a) show whole cell structures surrounded by whole coccoliths; treatment converts them to an assembly of coccolith fragments, as seen in Figure 2b. The ^{13}C CPMAS spectrum of the treated sample (Figure 1b) clearly indicates the overall reduction of the bioorganic matter. In particular, comparing the insets of Figure 1a and b, a substantial reduction of amides peptide peak is noted. As a result, the relatively narrow carbonate peak is exposed and clearly observed. Qualitatively, the ^{13}C CPMAS spectra show that treatment efficiently removes peptides and proteins (>90%) and, somewhat less efficiently, other bioorganic constituents. An additional means to spectrally emphasize the carbonate component without sample treatment is by employing a longer CP contact time.[36] Such conditions select species with relatively long rotating-frame relaxation time ($T_{1\rho}$) and/or such with weaker dipolar couplings to hydrogen atoms. The ^{13}C CPMAS spectrum of the intact sample, conducted with 8 ms contact time, indeed shows (Figure 1c, inset) a partially resolved carbonate peak with line width similar to that of the treated sample (Figure 1b, inset). This similarity in carbonate peak positions and line widths between treated and intact samples confirms that the NaOCl treatment is not affecting the calcite carbonate environment.

Whereas the indirect excitation (CP) results in spectra biased to carbons with nearby hydrogen atoms, in order to monitor the crystalline environments and to quantitatively characterize them in the *E. huxleyi* samples, direct excitation (DE) was employed with several relaxation delay times. The ^{13}C DE spectra of the intact and treated samples (Figure 3) clearly exhibit a 168.6 ppm peak of the crystalline carbonate with narrow line width of ∼15(±1) Hz. ^{13}C DE experiments acquired with a 67 min relaxation delay showed ca. 20% signal intensity increase of the carbonate, implying that, for the bulk crystalline calcite carbonates, $T_1(^{13}\mathrm{C}) \approx 30$ min.[37] Interestingly, ^{13}C DE

(34) Veshtort, M.; Griffin, R. G. *J. Magn. Reson.* **2006**, *178*, 248–282.
(35) Massiot, D.; Fayon, F.; Capron, M.; King, I.; Le Calve, S.; Alonso, B.; Durand, J. O.; Bujoli, B.; Gan, Z. H.; Hoatson, G. *Magn. Reson. Chem.* **2002**, *40*, 70–76.
(36) Stejskal, E. O.; Memory, J. D. *High Resolution NMR in the Solid State: Fundamentals of CP/MAS*; Oxford University Press: New York, 1993.
(37) T_1 is calculated numerically solving the carbonate intensity ratio at the two time points: $I(t_1 = 67\ \mathrm{min})/I(t_2 = 40\ \mathrm{min}) = [1-\exp(-67/T_1)]/[1-\exp(-40/T_1)] = 1.20$.

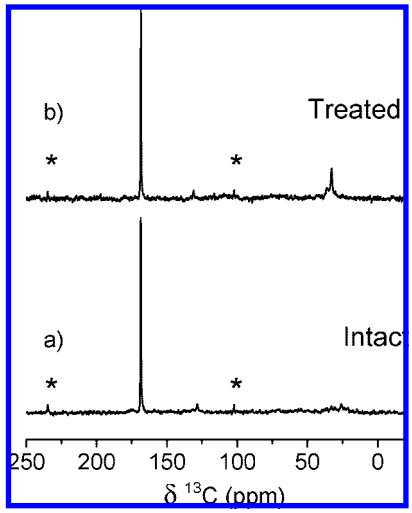

Figure 3. 75.5 MHz ^{13}C DE NMR spectra of *E. huxleyi* samples. (a) Intact and (b) treated. The calcite carbonate peak at 168.6 ppm is the dominant peak. A relaxation delay of 40 min was employed. Spinning sidebands are denoted by ∗.

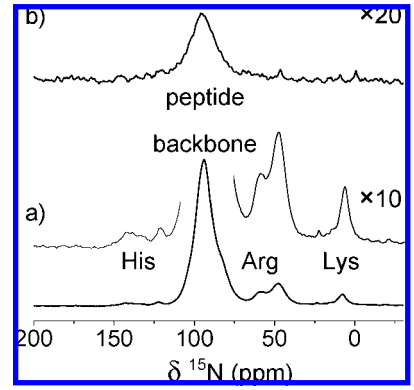

Figure 4. 30.4 MHz ^{15}N CPMAS NMR spectra of *E. huxleyi*. (a) Intact sample with predominantly protein/peptide peaks and (b) treated sample with predominantly residual peptide backbone peak. 80% of the nitrogen content is removed.

spectra acquired using a 20 s relaxation delay recovered as much as 18% and 15% (data not shown) of the total carbonate intensity obtained by the 40 and 67 min relaxation delays, respectively. These carbonates, reported via the short relaxation delay experiments, must therefore originate in environments with much shorter T_1(^{13}C) relaxation times compared to those of the typical crystalline carbonates.[38] We make a simplified assumption that there are just two carbonate populations and the fast-relaxing component is fully reported in the 20 s relaxation delay measurement. Under this assumption, T_1(^{13}C) of the slow-relaxing crystalline calcite carbonates is recalculated, giving a lower limit estimate of 35 min.[39] While the quantitative evaluation of T_1(^{13}C) may be further refined, it is expected to introduce only a small correction. A 40 min relaxation time was reported by low-field (8.5 MHz ^{13}C) calcite single-crystal measurements.[40] Therefore, as a practical choice, we employed a 40 min relaxation delay in collecting the quantitative DE spectra. Under the above simplified assumption of only two distinct crystalline environments being present, the full carbonate intensity is 1.38 times the intensity obtained at 40 min.[41] Of the corrected total carbonate count, 13% is the fast-relaxing population.

The ^{13}C DE spectra reconfirm the high efficiency of bioorganic content removal, in particular peptides, by the treatment, as seen by the CP spectra. Moreover, the spectra clearly demonstrate the high content of the inorganic calcium carbonate in the samples. Deconvolution of the various peaks in each of the two spectra applying the 1.38 correction factor indicates that ^{13}C carbonate is greater than 65% of the entire carbon content. Furthermore, using the two techniques, i.e., CP to enhance carbon moieties in proton-rich environments and DE to emphasize the overwhelming inorganic crystalline carbonate, provides experimental selectivity where inorganic vs organic components are clearly evident. Further scrutiny of the above data shows that the line width of the carbonate peak exposed by CP is about 4-fold larger than that depicted by the DE experiment: 65 Hz vs 15 Hz, respectively. The different characteristic line widths between carbonate environments are indicative of a heterogeneous chemical environment detected by the CP and a chemically unique environment detected by the DE measurements. This distinction further substantiates the selective identification of the two environments: a highly ordered bulk crystalline environment exposed by DE (narrow peak), in contrast to the less ordered, heterogeneous interfacial environment exposed by CP (broad peak). The identification of the latter as interfacial carbonates can be rationalized by the presence of proximate bioorganic molecules at the interface, from which cross-polarization originates. As the crystalline environment is terminated and/or interrupted, heterogeneous chemical environments occur, as reflected by the broad CP carbonate line width. Similar observations were reported for synthetic calcites with incorporated organic molecules.[28,42−44]

In addition, comparing the spectral features of the carbonate peak of the intact vs the treated samples, no changes of line widths or peak positions occur. In particular, the fact that the CP carbonate peak remains unchanged (just better resolved in the treated sample) implies that bioorganic interfacial matter was not removed by the NaOCl treatment: both interfacial and bulk $CaCO_3$ remain intact.

Nitrogen and Phosphorus Content in *E. huxleyi* Samples. In order to further characterize the bioorganic matter, both ^{15}N and ^{31}P CPMAS spectra were recorded for the intact and treated samples, as shown in Figures 4 and 5. The ^{15}N CPMAS NMR spectrum of the intact sample (Figure 4a and its inset) depicts typical protein peaks, with the main amide backbone peak at ca. 94.0 ppm, ε-lysine nitrogen at 7.6 ppm, and arginine guanidinium nitrogens at 49.2 and 57.4 ppm (terminal and internal, respectively). Histidine side chains, and possibly

(38) Nassif, N.; Pinna, N.; Gehrke, N.; Antonietti, M.; Jager, C.; Colfen, H. *Proc. Natl. Acad. Sci. U.S.A.* **2005**, *102*, 12653–12655.
(39) Considering a fixed contribution of the fast-relaxing component, the re-evaluated intensities of the slow-relaxing component at 67 and 40 min yield the ratio I(67 min)/I(40 min) = 1.25. Solving the above expression for this ratio yields T_1 = 35 min.
(40) Lauterbur, P. C. *Phys. Rev. Lett.* **1958**, *1*, 343–344.
(41) The total carbonate intensity at 40 min relaxation delay measurements is corrected to account for incomplete relaxation as follows. (1) Calculating the fully relaxed intensity of the 0.82 slow-relaxing population: $I_{slow}(40\ min) = I_{slow(eq)}[1-\exp(-t/T_1)] = I_{slow(eq)}0.68$, with T_1 = 35 min and t = 40 min. (2) Adding the 0.18 fast-relaxing population to yield the total carbonate intensity: $I_{T(eq)} = [0.18 + 0.82/0.68]I_{T(40\ min)} = 1.38I_{T(40\ min)}$.
(42) Phillips, B. L.; Lee, Y. J.; Reeder, R. J. *Environ. Sci. Technol.* **2005**, *39*, 4533–4539.
(43) Feng, J.; Lee, Y. J.; Reeder, R. J.; Phillips, B. L. *Am. Mineral.* **2006**, *91*, 957–960.
(44) Mason, H. E.; Frisia, S.; Tang, Y.; Reeder, R. J.; Phillips, B. L. *Earth Planet. Sci. Lett.* **2007**, *254*, 313–322.

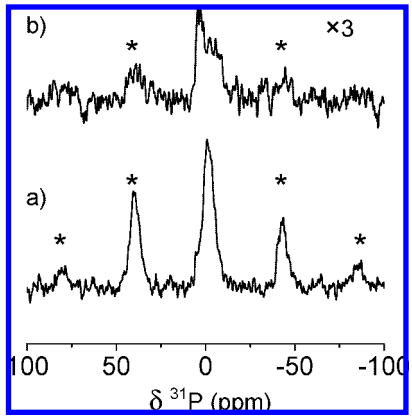

Figure 5. 121.5 MHz ^{31}P CPMAS NMR spectrum of *E. huxleyi* samples. (a) Intact and (b) treated. Treatment removed ca. 80% of the intact sample phosphorus content. Spinning sidebands are denoted by ∗.

contributions from DNA bases, give rise to the complex peaks in the 122−143 ppm chemical shift region. The ^{15}N CPMAS NMR spectrum of the treated sample (Figure 4b) mainly shows a residual peptide backbone peak. The ^{31}P CPMAS NMR spectrum of the intact sample (Figure 5a) reveals a broad, unresolved peak that may arise from various contributions, e.g., inorganic phosphate, DNA phosphoesters, and phosphorylated proteins. Upon NaOCl treatment, a smaller ^{31}P peak is observed (Figure 5b), yet with a different spread of heterogeneity relative to the peak in the spectrum in Figure 5a. Hence, upon NaOCl treatment, the ^{15}N and ^{31}P spectra show removal of up to 80% of N- and P-containing bioorganic matter, similar to the above ^{13}C results.

***E. huxleyi* Calcite REDOR NMR Characterization.** In the following, our goal is to refine the characterization of the biomineralized *E. huxleyi* calcite, identify its composition and the resulting organic−inorganic interactions. For that purpose, REDOR NMR[33] is employed. REDOR is a dipolar recoupling technique that enables selective identification of calcite carbonates with adjacent phosphorus and/or nitrogen moieties. As earlier literature postulates the embedment of peptides and/or proteins within the crystalline material,[24−26,28] REDOR would be best suited to probe such putative bioorganic−inorganic interfacial interactions. Since natural abundance levels do not yield sufficient sensitivity, the ^{13}C and ^{15}N enrichment makes this technique feasible in this study. The ^{13}C REDOR experiment is performed in two steps: first, without dipolar recoupling, producing a reference spectrum, S_0, with all ^{13}C species reported; second, reintroducing dipolar coupling with, e.g., ^{15}N nuclei, producing the recoupled S_R spectrum. In the latter, peaks of carbon species with proximate ^{15}N atoms, up to 5 Å apart, are attenuated compared to the reference spectrum. This attenuation of spectral peaks provides (a) spectral editing capability, often manifested by the difference spectrum, $\Delta S = S_0 - S_R$, exclusively exhibiting peaks of C species with adjacent N moieties,[45,46] and (b) geometrical information, e.g., the strength of the dipolar coupling and the internuclear distance can be determined by varying the length of the REDOR dipolar evolution period (the number of rotor periods).[47,48] ^{13}C REDOR

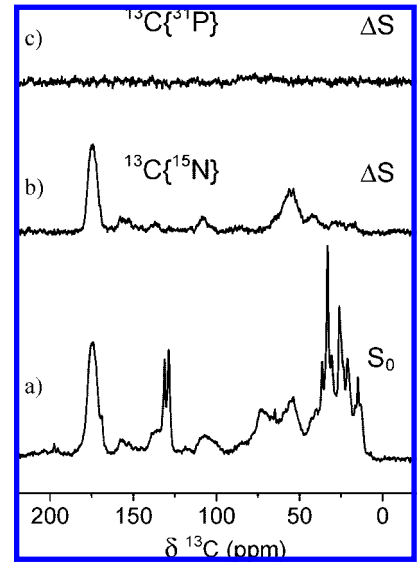

Figure 6. 75.5 MHz ^{13}C CPMAS $16T_R$ REDOR NMR spectra of the intact *E. huxleyi* sample. Difference spectra are drawn normalized relative to their respective reference spectra: (a) REDOR S_0 reference spectrum, (b) ^{13}C{^{15}N} REDOR ΔS spectrum, and (c) ^{13}C{^{31}P} REDOR ΔS spectrum.

was applied using both excitation schemes, allowing a selective probe of either the interfacial region via CP or the bulk crystalline using DE.

Interfacial Calcite: Cross-Polarization REDOR NMR. The ^{13}C{^{15}N} $16T_R$ CP-REDOR S_0 and ΔS spectra of the intact sample are shown in Figure 6a and b, respectively. The reference REDOR spectrum, S_0, is similar to that shown in Figure 1a. Given the short dipolar evolution time of $16T_R$ (3.2 ms), the difference spectrum, ΔS, shows peaks for carbon species with a nitrogen atom within 4 Å distance. Focusing on the carbonyl region, this spectrum (Figure 6b) shows a strong difference peak of the amide carbonyl. This observation serves as an internal experimental REDOR validation, confirming both the identification of the peak as a peptide backbone peak and the high level of ^{15}N labeling: most amide carbons possess an adjacent (one-bond) ^{15}N-amide nitrogen neighbor. This $16T_R$ CP-REDOR spectrum shows no difference peak for the small, partially resolved carbonate peak. Conducting the $16T_R$ CP-REDOR measurements on the treated sample, for which the carbonate peak is better resolved, also resulted in no carbonate difference peak (data not shown). Similarly, the analogous ^{13}C{^{31}P} $16T_R$ CP REDOR difference spectrum (ΔS, Figure 6c), shows no carbonate difference peak. The above REDOR measurements therefore imply that interfacial carbonates do not possess proximate nitrogen or phosphorus atoms within 4 Å. On the basis of the above observations, the abundant occurrence of such proximities to interfacial carbonates is excluded; if such interfacial interactions occur, their abundance must be below our experimental detection limits (<5% for cross-polarization experiments).

Bulk Crystalline Calcite: Direct Excitation REDOR NMR. In order to focus the characterization on the bulk crystalline carbonate environment, DE-REDOR was employed using two different relaxation delays, 20 s and 40 min, hence yielding

(45) Kaustov, L.; Kababya, S.; Du, S. C.; Baasov, T.; Gropper, S.; Shoham, Y.; Schmidt, A. *Biochemistry* **2000**, *39*, 14865–14876.
(46) Kaustov, L.; Kababya, S.; Belakhov, V.; Baasov, T.; Shoham, Y.; Schmidt, A. *J. Am. Chem. Soc.* **2003**, *125*, 4662–4669.
(47) Mehta, A. K.; Shayo, Y.; Vankayalapati, H.; Hurley, L. H.; Schaefer, J. *Biochemistry* **2004**, *43*, 11953–11958.
(48) Paik, Y.; Yang, C.; Metaferia, B.; Tang, S. B.; Bane, S.; Ravindra, R.; Shanker, N.; Alcaraz, A. A.; Johnson, S. A.; Schaefer, J.; O'Connor, R. D.; Cegelski, L.; Snyder, J. P.; Kingston, D. G. I. *J. Am. Chem. Soc.* **2007**, *129*, 361–370.

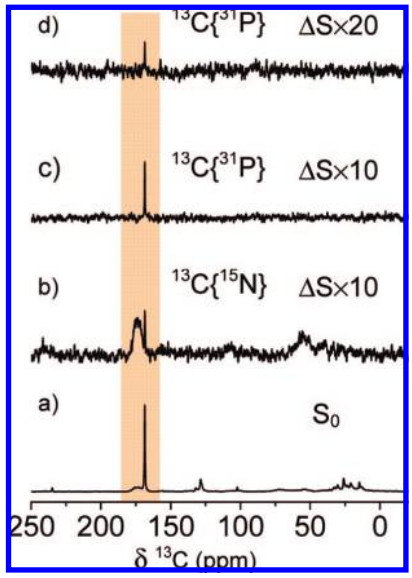

Figure 7. 75.5 MHz 16T_R ^{13}C DE-REDOR NMR spectra of the intact *E. Huxleyi* sample. Difference spectra are drawn normalized relative to their respective reference spectra: (a) $^{13}C\{^{15}N\}$ REDOR S_0 reference spectrum, (b) $^{13}C\{^{15}N\}$ REDOR ΔS spectrum, and (c) $^{13}C\{^{31}P\}$ REDOR ΔS spectrum. A 20 s relaxation delay was employed for spectra a−c. (d) $^{13}C\{^{31}P\}$ REDOR ΔS spectrum with relaxation delay 40 min. The carbonate calcite peak is at 168.6 ppm, with 15 Hz line width, in the four spectra.

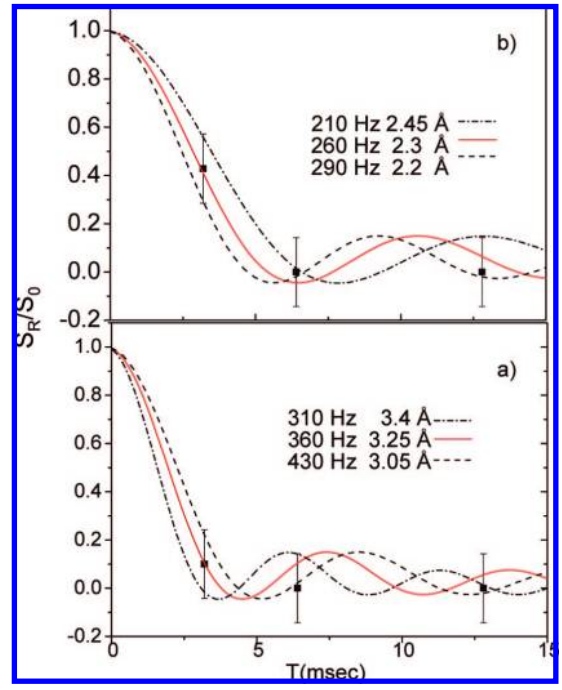

Figure 8. S_R/S_0 REDOR curves: (a) $^{13}C\{^{31}P\}$ and (b) $^{13}C\{^{15}N\}$ DE-REDOR. Experimental data (■) and error bars as a function of dipolar recoupling time for *E. huxleyi* calcite carbonate carbon interactions with N and P atoms in structural defects. Simulations: best-fit (continuous line) and error limits (dotted lines). Simulations were done using SpinEvolution.[34]

spectra that emphasize either the fast- or the slow-relaxing environments, respectively.

The $^{13}C\{^{15}N\}$ 16T_R DE-REDOR reference and difference spectra of the intact sample employing a 20 s repetition delay are shown in Figure 7a and b, respectively. The reference spectrum in Figure 7a is similar to that shown in Figure 3a, yet due to the short relaxation delay (20 s), all species with shorter T_1, e.g., bioorganic carbons, are overemphasized relative to the partially relaxed carbonates. The DE-REDOR difference spectrum in Figure 7b clearly shows the broad amide carbonyl peak (centered at 175 ppm), similar to that observed in the CP-REDOR (Figure 6b). Interestingly, a pronounced calcite carbonate REDOR difference peak appears (168.6 ppm; Figure 7b). An even more pronounced carbonate peak is depicted by the $^{13}C\{^{31}P\}$ 16T_R DE-REDOR difference spectrum in Figure 7c. Both observations clearly demonstrate that within the bulk crystalline calcite there are carbonates which possess proximate nitrogen and phosphorus moieties. The narrowness of the difference REDOR peaks in both cases (<15 Hz), and the fact that their chemical shift position remains as in the reference spectra, indicate that these peaks report structurally unperturbed crystalline calcite carbonates adjacent to defect sites. The N/P moieties adjacent to these carbonate sites may therefore be small anionic moieties that fit into lattice sites and introduce minute or no lattice distortion. The possibility that these could be large moieties, such as organic molecules, peptides, or proteins (phosphorylated), is excluded. The presence of bioorganic moieties would have led to local structural distortions that would cause also chemical shift changes and heterogeneous line broadening and give rise to CP signals due to their hydrogen-rich environment. Effects of this kind are clearly depicted by the broad interfacial carbonate line width in the ^{13}C CP spectra and are also documented in the literature.[28]

Internuclear REDOR-Determined Distances. In order to estimate the carbonate C···P and C···N internuclear distances within the crystalline defect sites, DE-REDOR with varying dipolar recoupling periods was applied to the intact *E. huxleyi* sample. The $^{13}C\{^{31}P\}$ DE-REDOR experiments (20 s relaxation delay) with 16-, 32-, and 64T_R produced S_R/S_0 values of 0.94, 0.93, and 0.93 ± 0.01, respectively.

This observation of calcite carbonates with adjacent phosphorus moieties reaching full dephasing at a value of 0.93 has an important implication: these constitute a subpopulation of 7 ± 1% of the carbonates reported by the 20 s relaxation delay spectrum. Moreover, the fact that full dephasing is already reached at 1.6 ms (16T_R) enables quantitative analysis of the S_R/S_0 data in order to derive an upper limit estimate for the C···P internuclear distance within this 7% subpopulation. Analyzing the data of this subpopulation on its own, the experimental data points between 1.00 and 0.93 are converted to a full REDOR dephasing scale, 1.0 to 0.0, and are fitted with a calculated REDOR evolution curve,[34] as plotted in Figure 8a. Solid squares and vertical bars represent the experimental data points and their respective errors. The continuous line represents a best-fit simulation of a REDOR evolution curve for a C···P dipolar-coupled spin pair with a coupling strength of 360 Hz, corresponding to $r_{[C\cdots P]}$ of 3.25 Å. The two additional simulated curves (dashed) represent C···P dipolar coupling strengths of 310 and 430 Hz, which correspond to $r_{[C\cdots P]}$ of 3.4 and 3.05 Å, respectively, with these distances encompassing the experimental error. Hence, the resulting $r_{[C\cdots P]}$ distance of 3.3 ± 0.2 Å represents an upper limit estimate under the assumption that only isolated spin pairs of the $^{13}C\cdots^{31}P$ nuclei occur within the crystalline material. This assumption is in accordance with the identification of these defects to be caused by the sparse incorporation of small moieties without the introduction of chemical shift changes. Examination of the treated sample via DE-REDOR as above yields similar dipolar evolution (data not shown), hence implying that the treatment has not altered the bulk crystalline material nor its phosphorus level.

Similarly, turning now to obtain an estimate for the carbonate C···N internuclear distance within the crystalline defect sites, $^{13}C\{^{31}N\}$ DE-REDOR was employed using a 20 s relaxation delay. S_R/S_0 dephasing values of 0.96, 0.93, and 0.93 ± 0.015 were obtained for 16-, 32-, and $64T_R$, respectively, and are shown in Figure 8b (■). Full REDOR dephasing is reached at $32T_R$ and at a level of 0.93. Also here, using the short relaxation delay time (20 s) of the fast-relaxing carbonates, the fraction of carbonates with a neighboring N-moiety is 7 ± 2%. The estimated internuclear C···N distance is obtained as above for C···P by fitting the experimental data with a calculated REDOR dephasing curve (continuous line, Figure 8), giving rise to a coupling strength of 260 Hz and $r_{[C\cdots N]}$ of 2.3 Å. Margins of error are flanked by two calculated dephasing curves (dashed lines, Figure 8b) with C···N dipolar coupling of 290 and 210 Hz for $r_{[C\cdots P]}$ of 2.2 and 2.45 Å, respectively. Hence, the resulting $r_{[C\cdots P]}$ distance of 2.3 ± 0.2 Å represents an upper limit estimate under the assumption that these $^{13}C\cdots^{15}N$ correspond to isolated and sparse nuclei pairs within the crystalline material. Examining the treated sample via DE-REDOR as above yields similar dipolar evolution, i.e., similar internuclear distances (data not shown). This observation further establishes the fact that the treatment has not altered the bulk crystalline material, nor its nitrogen content.

REDOR-Estimated Abundance of Carbonates Adjacent to P/N Defect. As shown above, the carbonate content reported by the DE spectra with the short relaxation delay, 20 s, is ca. 18% of the 40 min relaxation delay spectra. Hence, a quantitative estimate of the fraction of the crystalline sites with phosphorus moieties can be obtained. $^{13}C\{^{31}P\}$ DE-REDOR experiments with 16- and $64T_R$ were conducted using a 40 min relaxation delay. The difference spectrum of the latter (Figure 7d) clearly shows a small carbonate peak whose analysis gives rise to a S_R/S_0 of 0.98 ± 0.007. This observation indicates that up to ca. 2 ± 1% of the crystalline carbonates reported by the 40 min measurements possess a phosphorus neighbor. Correcting for the incomplete relaxation ($S_0 \rightarrow S_0 \times 1.38$) sets the estimated upper limit value for the defect concentration at 1.4%. The observation that 7% P-neighboring carbonates are found via the 20 s relaxation delay experiments, while their overall concentration is below 1.4%, implies that carbonates next to phosphorus defect sites reside exclusively in the short T_1 environments (Figure 7c); *vice versa*, most of the carbonates adjacent to defect sites are reported in the short relaxation delay experiments. In turn, this observed T_1 shortening effect is straightforwardly rationalized in view of the nature of the defect site, namely, the presence of a ^{31}P or $^{15}N/^{14}N$ in the lattice (with their dipole−dipole, CSA, or quadrupole interactions), and the reduced local order leading to reduced rigidity around the defect site; both can create efficient relaxation mechanisms.[49]

The $^{13}C\{^{15}N\}$ DE-REDOR experiment with a 40 min repetition delay quantifies the fraction of the crystalline carbonates with adjacent nitrogen moieties as 2 ± 1%, residing preferentially in a short T_1 environment, similar to the identified fraction of carbonates with proximate phosphorus moieties. An estimate of the maximum carbonate concentration adjacent to N-defects of 1.4% is obtained by correcting the REDOR S_0 data to account for the incomplete carbonate relaxation.

(49) Spiess, H. W. *NMR Basic Principles and Progress*; Springer Verlag: New York, 1978; Vol. 15.

Low Nutrient Medium. Low nutrient conditions were reported to stimulate liths production,[19,20,50,51] and this motivated us to examine the resulting calcite under such growth conditions. Throughout this study, the growth of *E. huxleyi* under conditions of low nutrient concentration, f/50 medium, was explored in parallel with growth in f/2 medium. Analogous MAS NMR experiments (CP- and DE-REDOR) and microscopy, as done for samples obtained from f/2, were performed for f/50 samples, both intact and treated. Qualitatively, these samples yielded similar results, identifying crystalline calcite with phosphorus and nitrogen defect sites, yet with concentrations even slightly higher than those observed for the f/2 samples. The large concentration difference of the nutrients and the similarity of the resulting biomineral may further reflect that the P/N incorporation process is a controlled one, directed by the cellular function and regulation within the coccoliths-forming Golgi-derived vesicles.[52] Only the implications important for the current study were noted. Future work will aim to finely monitor the effects incurred on the forming biomineral by variations of environmental conditions.

Discussion

Growth of *E. huxleyi* in a medium enriched by 98% ^{15}N and 25% ^{13}C enabled high sensitivity solid-state NMR examination and characterization of both its bioorganic and biomineral components *in situ*. Cultures were harvested with minimal interference in an attempt to minimize any alterations of the biogenic calcite or bioorganic matter adhered to it. Therefore, these intact samples still contained excess biological matter. In order to reduce the excess bioorganic content that may obscure desired spectroscopic details and to better focus on the calcite (carbonate) and its interfacial regions, harvested cultures were treated with a short, delicate exposure to NaOCl (2.5%). Studying samples from both preparation procedures showed that the treatment removed most excess bioorganic matter (ca. 80%) without affecting crystalline or interfacial calcite coccoliths.

Our NMR measurements directly probed and delineated the different structural/chemical carbonate environments within the calcite, both bulk crystalline and interfacial regions, and enabled detailed *in situ* identification of the biomineralized calcite structure and composition, as produced by the biological system. The calcite carbonate peak identified at 168.6 ppm, in both the crystalline and interfacial environments, is in agreement with earlier reports.[42,53,54] NMR monitoring of its line width, relaxation properties (T_1), and the interactions of carbonates with "foreign" moieties within the calcite via REDOR NMR renders the carbonate a most powerful reporter of its local environment.

The carbonate in the crystalline calcite environment is reported by direct excitation NMR techniques, where its very narrow line width is indicative of a highly ordered environment that is structurally and chemically unperturbed. The carbonate carbon in this crystalline environment has a long $T_1(^{13}C)$ relaxation time, ca. 35 min, in accordance with earlier literature reports,[40] indicative of a highly rigid crystal lattice. Within this highly rigid lattice, we identify carbonate environments with a

(50) Stoll, H. M.; Rosenthal, Y.; Falkowski, P. *Geochim. Cosmochim. Acta* **2002**, *66*, 927–936.
(51) Wahlund, T. M.; Zhang, X. Y.; Read, B. A. *Micropaleontology* **2004**, *50*, 145–155.
(52) Outka, D. E.; Williams, D. C. *J. Protozool.* **1971**, *18*, 285−&.
(53) Sherriff, B. L.; Grundy, H. D.; Hartman, J. S. *Can. Mineral.* **1987**, *25*, 717–730.
(54) Papenguth, H. W.; Kirkpatrick, R. J.; Montez, B.; Sandberg, P. A. *Am. Mineral.* **1989**, *74*, 1152–1158.

substantially shorter $T_1(^{13}C)$, signifying an environment with reduced rigidity, yet with retained high structural order. The latter is implied by the unchanged carbonate peak position and line width. This short $T_1(^{13}C)$ crystalline calcite environment makes up ca. 13% of the entire calcite. Further scrutiny of this short $T_1(^{13}C)$ environment shows that, dispersed within it, 7 ± 1% of its carbonates are proximate to lattice defect sites with P or N small moieties. These constitute up to 1.4% of the entire calcite carbonate of the coccoliths of *E. huxleyi*. The unaltered peak position and narrow line width (REDOR ΔS peak <15 Hz) of carbonates proximate to P and N atoms means that these carbonates do not experience any local chemical changes nor structural distortions; the presence of these "foreign" atoms is manifested only by carbonate $T_1(^{13}C)$ shortening. Geometrical constraints for the carbonate C···N and C···P internuclear distances of 2.3 and 3.3 ± 0.2 Å, respectively, were determined by REDOR NMR experiments. In view of the above observations and analyses, these are identified unambiguously as *structural defect sites* within the crystalline calcite. This determination is further supported by studies where bioorganic molecules—citrate, glutamate, and aspartate—were incorporated in synthetic calcite by coprecipitation.[42] In these studies, a *broad* carbonate peak (~140 Hz) resulted from cross-polarization that originated in the bioorganic hydrogen atoms. Moreover, bicarbonate within synthetic calcite was reported to exhibit a distorted, heterogeneous local carbonate environment (~120 Hz line width) that is effectively detectable via cross-polarization from its single hydrogen.[43] In our study, if the REDOR-identified P and N species were components of small bioorganic molecules, cross-polarization would also have exposed a narrow carbonate peak. This is clearly not the case for the *E. huxleyi* calcite. Carbonates adjacent to true structural defects experience no chemical shift distortions. In contrast, carbonates adjacent to incorporated bioorganic molecules and carbonates at crystalline boundaries accommodate substantial structural perturbations and experience similar distortions, and we therefore classify the latter two environments as *interfacial*.

Moreover, the absence of a narrow carbonate peak component from the CPMAS spectra excludes the possibility that the foreign P and N moieties are protonated. The phosphorus-bearing moiety is most likely inorganic phosphate (PO_4^{3-}), quite commonly found in geological calcites such as speleothems[44] and shown in synthetic calcite coprecipitation studies.[55−57] For such cases, it has been shown that, in calcite, the incorporation of the PO_4^{3-} species occurs preferentially and this phosphate gives rise to a broad heterogeneous ^{31}P peak over the 3.1−3.7 ppm range. Our ^{31}P CPMAS spectra of both the intact and treated samples show a broad, unresolved peak with intensity over this ppm range; however, a definite assignment is not yet possible. As for the identity of the incorporated N moieties, nitrate anions (NO_3^-) are plausible. Studies of synthetic calcites with nitrate (and with chloride and sulfate) anions coprecipitated reported no detectable lattice distortions (fine distortions were observed upon sulfate incorporation).[58] These defects may be formed by a substitution of a carbonate moiety; however, according to the REDOR-derived distances, they are placed at a distance which is shorter than the shortest C···C distance of 4.05 Å.[59] Future efforts will aim to directly identify the included moieties.

Finally, the interfacial carbonates reported by the CPMAS spectra display a heterogeneously broadened peak, evenly spread around the original peak position (168.6 ppm). For these interfacial carbonates, the occurrence of close proximities to either N or P moieties, as identified within the crystalline calcite, is excluded. This fact implies that, given there exists a repetitive interaction pattern that stabilizes the interface by bioorganic matter, it does not consist of tightly bound peptides or proteins. Polysaccharides were reported to participate in calcite surface interactions.[60] Attempts to identify interactions with such hydrocarbons are deferred to our continuing work.

Conclusions

This study, utilizing solid-state NMR techniques in combination with biosynthetic stable isotope enrichment, provides for the first time direct observation of the molecular-level details of intact biomineralized calcite *in situ*, in particular that grown by the coccolithophore *E. huxleyi*. Quantitative evidence on the sparse incorporation of P and N inorganic moieties and their placement as structural components within the biogenic calcite lattice at tight geometries is clearly demonstrated. In spite of the incorporation of these inorganic moieties within the lattice at close proximities to the carbonate anions, they do not measurably alter the local chemical/electronic structure of the carbonates; the only detectable effect is the reduction of crystalline rigidity. The occurrence of such tight interfacial carbonate interactions with N- and/or P-containing biomolecules that may so form an interface stabilization motif is excluded. Maintaining very similar incorporation levels and geometries despite growth under P- and N-sufficient and -deficient conditions alludes to the high level of control and regulation exercised by *E. huxleyi* in constructing its calcite coccoliths.

The capability of *in situ* direct observation of such a small concentration of defect sites and identification of the minute effects exerted on their immediate environments are unique to solid-state NMR techniques alone. Such details are not amenable to any diffraction technique or other spectroscopy. This study, therefore, also demonstrates the power and importance of solid-state NMR for the investigation of such complex systems.

Acknowledgment. We thank Prof. Lia Addadi and Yael Politi from the Weizmann Institute of Science, Dr. Yeala Shaked from the Inter University Institute for Marine Sciences and Hebrew University in Jerusalem, and Dr. Yael Balazs from the Technion for stimulating and helpful discussions.

JA803985D

(55) Kanel, J. D.; Morse, J. W. *Geochim. Cosmochim. Acta* **1978**, *42*, 1335–1340.
(56) Tsenga, Y.-H.; Zhana, J.; Lina, K. S. K.; Moua, C.-Y.; Chan, J. C. C. *Solid State Nucl. Magn.* **2004**, *26*, 99–104.
(57) Hinedi, Z. R.; Goldberg, S.; Chang, A. C.; Yesinowski, J. P. *J. Colloid Interface Sci.* **1992**, *152*, 141–160.
(58) Kontrec, J.; Kralj, D.; Brecevic, L.; Falini, G.; Fermani, S.; Noethig-Laslo, V.; Mirosavljevic, K. *Eur. J. Inorg. Chem.* **2004**, 4579–4585.
(59) Maslen, E. N.; Streltsov, V. A.; Streltsova, N. R. *Acta Crystallogr. B* **1993**, *49*, 636–641.
(60) Marsh, M. E. *Protoplasma* **1999**, *207*, 54–66.